Permanent El Niño-Like Conditions During the Pliocene Warm Period
Michael W. Wara *et al.*
Science **309**, 758 (2005);
DOI: 10.1126/science.1112596

3A). In 23 recordings of individual samples from five separate membrane preparations, channel gating started within 2 min of irradiation at 366 nm in the absence of applied tension. The channel opened during this "on" state with a conductance of 0.5 to 1 nS, which increased to 1.5 nS after application of a pressure gradient [Supporting Online Material (SOM) Text]. UV-induced openings of the channels consistently start after a lag period. This delay in activation is consistent with a comparable 2-min time scale observed in the absorption spectra for the neutral-to-zwitterionic isomerization to reach completion (Fig. 2B). Once activated, however, the channels continue to work. If the patch is then irradiated with visible light, the channel activity drops substantially within seconds and the channels switch off. The rapid deactivation, contrasted with the slow activation, suggests a critical polarity (dependent on the number of switches in the zwitterionic MC form) necessary for ion conduction through the hydrophobic pore of the homopentamer channel. It is not yet clear how many charges are necessary to open the pore.

Irradiation of the closed channel with a second UV cycle follows the same pattern as in the first cycle, and, after a lag period, channel openings are evident from current flow. Figure 3B shows representative channel activity during the last 40 s of each irradiation period. There are many channel opening events during the first UV period, whereas there are no channel openings at the end of the visible light treatment. The lower number of channel openings on the second UV treatment compared with the first correlates with the lower amount of the zwitterionic MC form seen in the absorption spectrum (Fig. 2C) after the first cycle of illumination.

In order to test the utility of the light-addressable nanovalve in controlling the exchange of solutes other than ions across a membrane, we conducted classical efflux experiments with a liposomal system containing a self-quenching fluorescent dye, calcein. The use of such calcein-loaded liposomes to monitor the permeability of liposomal membranes is a long-standing practice in the field of liposomal drug delivery (29). Because of the high local concentration inside the liposomes, the fluorescence intensity of calcein is low, but release from these liposomes results in dilution of the dye and consequently a large increase in fluorescence signal. Here, we adapted this method to study the gating of MscL under isoosmotic conditions. We reconstituted the modified photoactive MscL into liposomes and analyzed the response of the fluorescence signal to activation of the channel. In the case of the unidirectional nanovalve **1b**, some slow dye leakage (10%) was observed under ambient conditions without specific light stimulation, but 366-nm irradiation resulted in 43% release of liposomal content on the same time scale (Fig. 4A). As expected, proteoliposomes containing unmodified MscL did not release dye irrespective of illumination, nor did liposomes without protein.

Similar light-induced release of calcein under isoosmotic conditions was observed for the reversible nanovalve (Fig. 4B). In this case, however, the amount released was lower compared with the one-way switch even though the reconstitution conditions were the same. The major difference between the two photosensitive molecules is their hydrophobicity, which is a key parameter for inducing spontaneous gating of this otherwise mechanosensitive channel. The calculated hydrophobicity of the reversible switch is higher than that of the one-way switch. These results are nonetheless a clear step toward a practical, photogated nanoscale delivery system.

References and Notes

1. B. L. Feringa, *Molecular Switches* (Wiley, New York, 2001).
2. K. Ichimura, S.-K. Oh, M. Nakagawa, *Science* **288**, 1624 (2000).
3. C. Bertarelli, A. Bianco, F. D'Amore, M. C. Gallazzi, G. Zerbi, *Adv. Funct. Mater.* **14**, 357 (2004).
4. J. H. Folgering, J. M. Kuiper, A. H. de Vries, J. B. Engberts, B. Poolman, *Langmuir* **20**, 6985 (2004).
5. M. V. Alfimov, O. A. Fedorova, S. P. Gromov, *J. Photochem. Photobiol. A* **158**, 183 (2003).
6. I. Willner, S. Rubin, *Angew. Chem. Int. Ed.* **35**, 367 (1996).
7. S. Sukharev, A. Anishkin, *Trends Neurosci.* **27**, 345 (2004).
8. N. Levina *et al.*, *EMBO J.* **18**, 1730 (1999).
9. C. C. Cruickshank, R. F. Minchin, A. C. Le Dain, B. Martinac, *Biophys. J.* **73**, 1925 (1997).
10. B. Ajouz, C. Berrier, A. Garrigues, M. Besnard, A. Ghazi, *J. Biol. Chem.* **273**, 26670 (1998).
11. C. Berrier, A. Garrigues, G. Richarme, A. Ghazi, *J. Bacteriol.* **182**, 248 (2000).
12. P. Blount, S. I. Sukharev, M. J. Schroeder, S. K. Nagle, C. Kung, *Proc. Natl. Acad. Sci. U.S.A.* **93**, 11652 (1996).
13. C. C. Hase, A. C. Le Dain, B. Martinac, *J. Membr. Biol.* **157**, 17 (1997).
14. P. Blount, M. J. Schroeder, C. Kung, *J. Biol. Chem.* **272**, 32150 (1997).
15. X. Ou, P. Blount, R. J. Hoffman, C. Kung, *Proc. Natl. Acad. Sci. U.S.A.* **95**, 11471 (1998).
16. K. Yoshimura, A. Batiza, M. Schroeder, P. Blount, C. Kung, *Biophys. J.* **77**, 1960 (1999).
17. E. Perozo, A. Kloda, D. M. Cortes, B. Martinac, *J. Gen. Physiol.* **118**, 193 (2001).
18. G. Chang, R. H. Spencer, A. T. Lee, M. T. Barclay, D. C. Rees, *Science* **282**, 2220 (1998).
19. S. Sukharev, M. Betanzos, C. S. Chiang, H. R. Guy, *Nature* **409**, 720 (2001).
20. E. Perozo, D. M. Cortes, P. Sompornpisut, A. Kloda, B. Martinac, *Nature* **418**, 942 (2002).
21. J. Gullingsrud, K. Schulten, *Biophys. J.* **85**, 2087 (2003).
22. K. Yoshimura, A. Batiza, C. Kung, *Biophys. J.* **80**, 2198 (2001).
23. M. Sukhareva, D. H. Hackos, K. J. Swartz, *J. Gen. Physiol.* **122**, 541 (2003).
24. A. Anishkin, C. S. Chiang, S. Sukharev, *J. Gen. Physiol.* **125**, 155 (2005).
25. Materials and methods are available as supporting material on *Science* Online.
26. C. G. Bochet, *J. Chem. Soc. Perkin Trans. 1* 125 (2002).
27. R. Reinhard, B. F. Schmidt, *J. Org. Chem.* **63**, 2434 (1998).
28. The hydrophilicity of the 22nd position of MscL determines the magnitude of tension required for channel opening (16). When glycine is replaced by cysteine, the higher hydrophobicity of cysteine stabilizes the closed state, and actuation requires a tension high enough to rapture the patch. The nitrophenyl derivative in modified MscL **1b** increases hydrophobicity even further. Therefore, we expect the channel not to open in the dark even if tension is applied up to the breaking point of the patch. However, upon illumination, the generation of charge at the same position leads to spontaneous opening in the absence of applied tension.
29. R. R. C. New, *Liposomes: A Practical Approach* (IRL Press, Oxford, 1990), pp. 105–161.
30. We thank the MscL team in Groningen for their contribution, B. Poolman and D. Stavenga for critical reading of the manuscript, the neurobiophysics group in University of Groningen for making available the patch clamp facilities, and the Netherlands Organization for Scientific Research (NWO-CW) (B.L.F.) and the Materials Science Centre (MSC plus), University of Groningen (M.W. and B.L.F), for financial support.

Permanent El Niño–Like Conditions During the Pliocene Warm Period

Michael W. Wara, Ana Christina Ravelo,* Margaret L. Delaney

During the warm early Pliocene (~4.5 to 3.0 million years ago), the most recent interval with a climate warmer than today, the eastern Pacific thermocline was deep and the average west-to-east sea surface temperature difference across the equatorial Pacific was only 1.5 ± 0.9°C, much like it is during a modern El Niño event. Thus, the modern strong sea surface temperature gradient across the equatorial Pacific is not a stable and permanent feature. Sustained El Niño–like conditions, including relatively weak zonal atmospheric (Walker) circulation, could be a consequence of, and play an important role in determining, global warmth.

The low-latitude Pacific Ocean provides a substantial portion of the global atmosphere's sensible and latent heat and is thus a central driver of climate (1). Over the past 25 years, the mean equatorial Pacific sea surface temperature (SST) has increased by ~0.8°C (2), possibly in response to increasing greenhouse gas concentration (3). Changes in the tropical Pacific mean climatic state may influence the amplitude of interannual, or El Niño–Southern

Oscillation (ENSO), climate variability (*4–7*), which may in turn play a role in global warming (*8*). The tropical Pacific mean state can be influenced by extratropical conditions, where surface water is subducted and flows into the tropical thermocline (the steep subsurface vertical thermal gradient between warm surface and cooler deep waters) (*4, 7, 9–12*). Conversely, the mean state of the tropical Pacific could be determined by changes in ENSO variability itself (*13, 14*). Overall, the mechanisms that control the mean state of the tropical Pacific are not fully understood, and predictions of future change in the mean state do not agree, probably because ENSO dynamics are not well-represented by most general circulation models (*15*). Thus, observational studies are needed to add additional constraints on the interplay between mean tropical conditions and global climate change.

Because instrumental (directly measured) records of climate change are relatively short (~100 years), geological records must be used to test theories that link long-term global climate change with tropical conditions (*7*). Characterizing conditions during times of global warmth requires investigation of older geologic periods that were substantially warmer than today. The most recent such interval is the Pliocene warm period [~4.5 to 3.0 million years ago (Ma)], which was characterized by ~3°C higher global surface temperatures relative to today (*16*). Although not a direct analogy of future transient global warming, the Pliocene warm period is a relevant natural experiment that can be used to understand processes contributing to long-term global warmth, because many boundary conditions were similar to today, including first-order ocean circulation patterns, the Earth's continental configuration, small Northern Hemisphere ice coverage, and atmospheric carbon dioxide concentrations (about 30% higher than pre-anthropogenic values) (*16*).

The equatorial west-to-east SST gradient and thermocline depth are intimately coupled parameters that exert a significant influence over both the mean state and variability of tropical Pacific climate (*4, 7*). Today, tropical trade winds drive ocean currents westward, resulting in a thick, warm, mixed layer and deep thermocline in the western equatorial Pacific (WEP) and a thin, warm, mixed layer and shallow thermocline in eastern equatorial Pacific (EEP). The trades also drive surface water divergence and upwelling of warm water in the WEP and cold water in the EEP, where the thermocline is deep and shallow, respectively. Thus, the trade winds cause a west-to-east, or zonal, asymmetry in thermo-

cline depth, SST (Fig. 1), and surface air pressure, which in turn strengthens the winds and further augments this asymmetry. The atmospheric circulation (Walker) cell, including easterly trade winds, rising air in the west, westerly winds aloft, and sinking air in the east, is a persistent feature of the tropical Pacific today; the magnitude of the zonal SST gradient is an excellent diagnostic of the strength of Walker circulation. Extreme temporary reductions in the zonal SST gradient and Walker circulation, or El Niño events, occur every 2 to 7 years and dramatically influence global climate by redistributing heat stored in the tropical Pacific to extratropical latitudes (*7, 15*). Likewise, changes in the long-term SST gradient may have altered extratropical conditions for sustained periods of time in the past (*17*) and could also potentially influence global climate in the future (*9*).

To represent the east-west Pacific SST gradient, we used the difference in SST and $\delta^{18}O$ between Ocean Drilling Program (ODP) site 806 in the WEP and ODP site 847 in the EEP (Fig. 1). Our sites are ideally located to monitor changes in equatorial upwelling and thermocline depth (away from the confounding effects of the Peru-Chile upwelling system). At each site, we made paired $\delta^{18}O$ and magnesium-to-calcium ratio (Mg/Ca) measurements on foraminiferal shells (a surface-dwelling species) to construct a time series of $\delta^{18}O$ and SST [using the calibration of Dekens *et al.* (*18*)], with an average sampling interval of 10 kyear from 5.3 Ma to present (*19*). The SST and $\delta^{18}O$ records, smoothed to remove glacial-interglacial variability, indicate that from 5.3 to 1.7 Ma the west-to-east difference in both parameters (Fig. 2, A and B) was relatively small: the west was ~2°C colder and the east ~2°C warmer than modern SSTs, and the west-to-east SST difference was al-

ways less than 2°C, with an average of 1.5 ± 0.9 (Fig. 2C). After 2.5 Ma, SST in the EEP began gradually decreasing. At 1.7 Ma, WEP temperatures warmed by ~2°C over a 50-kyear period, while the EEP continued to cool. By 1.6 Ma, the modern zonal SST difference of ~4°C, equivalent to a Mg/Ca contrast of 35%, was established. Thereafter, the EEP gradually cooled, and the mean west-to-east SST difference for the last 1.6 myear was 5.1 ± 0.9°C.

Our results contradict a recent study (*20*), using the same methodology and site selection (*19*), that concluded that the EEP was cooler (not warmer) in the early Pliocene. In the Rickaby and Halloran study (*20*), SST changes over the last 5 myear were represented by six data points, with only one data point from the Pliocene warm period interval, and we suspect that aliasing of higher frequency (orbital scale) variability led those authors (*20*) to erroneously conclude that the EEP was colder in the Pliocene warm period than at present. Our higher temporal resolution study, using over 400 data points over the last 5 myear, provides a more accurate reconstruction of mean SST trends and firm evidence for warm SSTs in the EEP during the Pliocene warm period. Furthermore, warmer-than-present alkenone-based SST estimates from the EEP (*21*) and foraminiferal $\delta^{18}O$ records (Fig. 2A) (*16, 22, 23*) indicating reduced hydrographic differences across the Pacific during the Pliocene warm period are consistent with the interpretations of our Mg/Ca records (Fig. 2C).

To track changes in the mean thermocline depth at the EEP site, we used $\Delta\delta^{18}O$, the difference in $\delta^{18}O$ between surface-dwelling *Globoritalia sacculifer* (without sac) and *G. tumida* (355 to 425 μm) (Fig. 2A), which occupies the base of the photic zone (at ~100 m

Ocean Sciences Department, University of California, Santa Cruz, CA 95064, USA.

*To whom correspondence should be addressed. E-mail: acr@es.ucsc.edu

January-December, 1968-1996
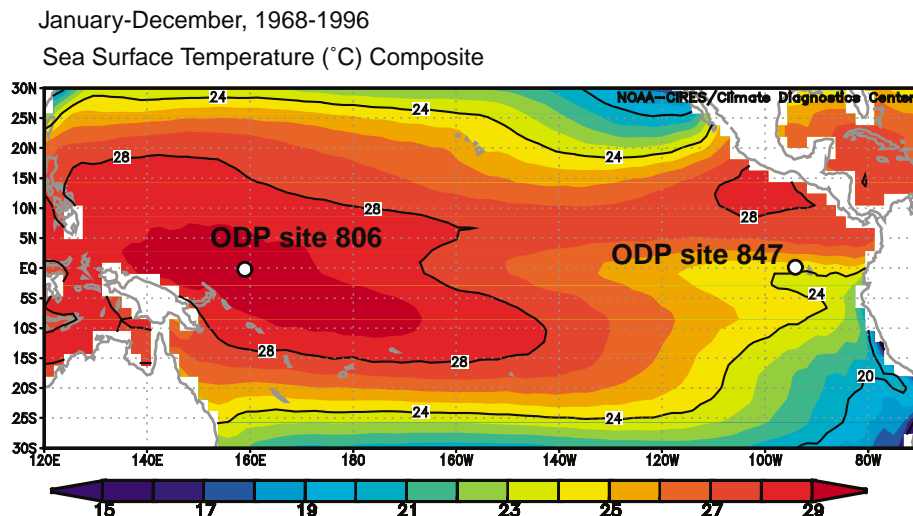Sea Surface Temperature (°C) Composite

Fig. 1. Sites used in this study, ODP site 847 (0°N, 95°W, 3373-m water depth) and ODP site 806 (0°N, 159°E, 2520-m water depth), overlaid on a map of climatological mean SSTs in the tropical Pacific Ocean (*36, 37*).

depth) (24, 25). Because there is a weak vertical salinity gradient in the EEP today, we assume that Δδ18O, on first order, represents the difference in temperature [ΔT between the surface and ~100m (Fig. 2D)]. High ΔT indicates that the cool thermocline water was shallow and above the base of the photic zone, whereas low ΔT indicates that cool thermocline water was deep and below the base of the photic zone. The increase in Δδ18O of ~1.2 per mil (‰) (Fig. 2A) equates to an increase in ΔT of ~5°C (26) (Fig. 2D), indicating the presence of a warmer or deeper thermocline in the beginning of the Pliocene, significant shoaling or cooling of the thermocline from 5.3 to 3.5 Ma, and relatively constant conditions from 3.5 Ma to present.

Previous work, which supports our thermocline reconstructions, indicates that δ18O differences between depth-stratified foraminiferal species (22, 27), foraminiferal species assemblages (27), which are strongly correlated to thermocline depth (25), and Mg/Ca-derived subsurface temperatures (20) were

similar on opposite sides of the basin during the warm Pliocene and became dissimilar by ~3.5 Ma. Taken together with our Mg/Ca-based evidence for a reduced west-to-east SST difference, these data indicate that the Pliocene warm period was not characterized by the typical west-to-east asymmetric conditions of the modern equatorial Pacific (Fig. 1). Rather, the Pliocene warm period had permanent El Niño–like conditions in several important aspects: Relative to today, the equatorial upwelling region of the EEP was warmer (Fig. 2B), the west-east SST difference along the equator was reduced (Fig. 2C), the thermocline in the EEP was deeper (Fig. 2D), and subsurface conditions were more symmetric across the tropical Pacific (20, 27). These observations are consistent with each other: A warmer and/or deeper thermocline would have resulted in warmer SSTs in EEP upwelling regions and reduced zonal SST and surface air pressure gradients. The reduced pressure gradient would have caused the winds and Walker circulation to slacken, thereby re-

inforcing the effects of warmer thermocline waters (28). Weak Walker circulation would have influenced the position and intensity of extratropical high- and low-pressure centers (29) and therefore would have had far-reaching climatic effects. In fact, the global expression of Pliocene warmth resembles the teleconnection pattern of El Niño (30).

The observed El Niño–like mean state during the Pliocene warm period could be related to changes in the mean state of extratropical regions (7). Theoretically, reduced subtropical SST (11) or surface salinity (12) gradients could have resulted in a warmer and/or deeper tropical thermocline and, consequently, warm water upwelling in the EEP. Although there is observational evidence for warmer subtropical SSTs (31), more detailed information on subtropical SST and salinity gradients is needed. Alternatively, the mean state could have been influenced by processes within the tropics, such as changes in the character of short-term (ENSO) variability (13, 14) perhaps due to the slightly different global boundary conditions, such as atmospheric CO_2 concentrations, of the early Pliocene compared to today.

Our sites alone cannot be used to determine whether the strong north-south SST gradients (Fig. 1) changed over time; future work detailing the spatial patterns of the tropical Pacific conditions could be used to test theories of what may have caused observed changes in equatorial conditions. In addition, future studies that try to differentiate between extratropical and within-tropical impacts on the mean state of the tropical Pacific should consider that several eastern boundary regions (California, Peru-Chile, West African margins), where cool upwelling occurs today, were significantly warmer before ~ 3 Ma (21, 32), suggesting that the thermocline was deeper and/or warmer globally, and not just in the tropical Pacific.

The difference in timing between the decrease in thermocline depth before ~4.0 Ma (Fig. 2D) and the increase in zonal SST difference at ~1.7 Ma (Fig. 2C) could be explained by several factors. First, because the thermocline depth proxy, Δδ18O, depends on the δ18O of G. tumida, which has a depth ecology at the base of the photic zone at ~100 m, it may not have been sensitive to additional shoaling above 100 m, which could have occurred after 4.0 Ma. Second, changes in salinity (and associated δ18O) of subsurface water could have a secondary effect on δ18O; thus, the effect of an increase in ΔT on δ18O after 4.0 Ma could be masked by a synchronous decrease in salinity of subsurface water. Detailed records of paired Mg/Ca and δ18O measurements on G. tumida are needed to better assess ΔT (33). And third, thermocline depth and SST are not linearly related (4), because the air-sea feedbacks that cause changes in Walker circulation become stronger as the ther-
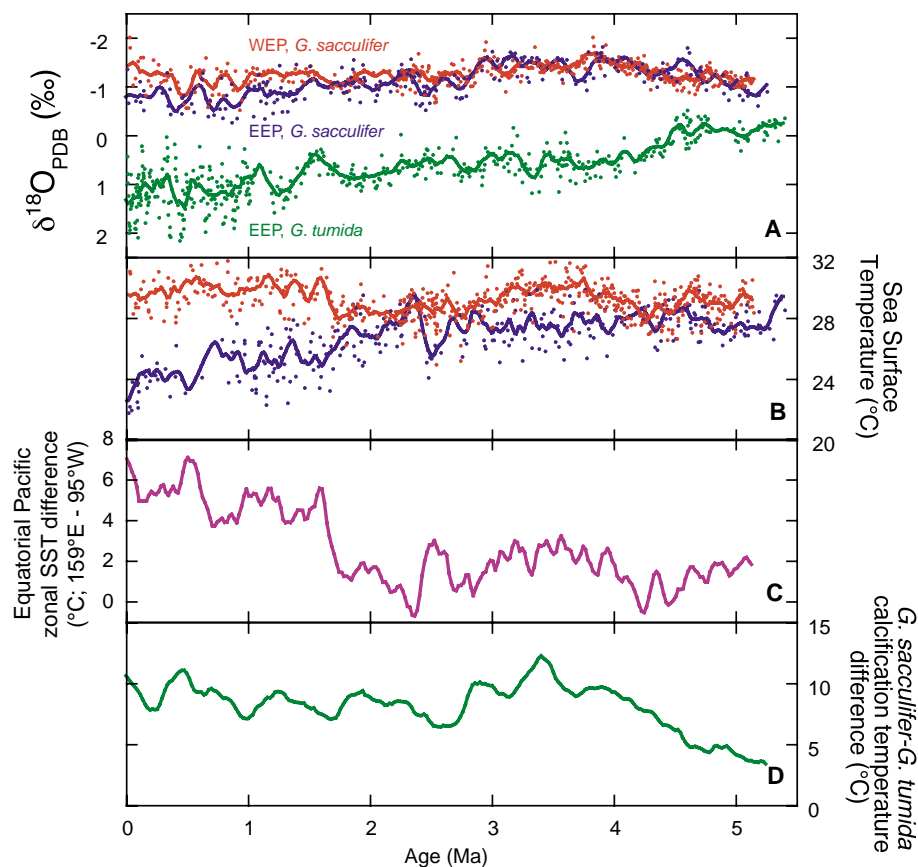

Fig. 2. Equatorial Pacific isotopic and temperature records. (**A**) oxygen isotope records of *G. sacculifer* (without sac, 355 to 425 μm) at ODP site 847 (blue) and 806 (red) as well as of *G. tumida* (355 to 425 μm) at ODP site 847 (green). (**B**) SSTs estimated from Mg/Ca measurements in *G. sacculifer* (without sac) from sites 847 (blue) and 806 (red). (**C**) The estimated zonal SST gradient on the equator between 159°E and 95°W. (**D**) The difference (Δ°C) between the calcification temperatures of *G. sacculifer* (without sac) and *G. tumida* at site 847 calculated by assuming that the difference between their δ18O entirely reflects temperature and that Δδ18O/0.21 = Δ°C. Heavy lines in all figures represent a 0.2-Ma Gaussian weighted running mean. Curves in (C) and (D) were calculated by using the smooth curves in (A) and (B).

mocline shoals. Thus, the increase in the zonal SST difference after ~1.7 Ma could indicate that tropical air-sea feedbacks (34) amplified the SST response to a changing thermocline once critical thermocline conditions were reached.

Mean tropical thermocline conditions can influence air-sea feedbacks that affect high-frequency climate variability (4, 15); the amplitude of ENSO variability is dampened when the thermocline is deeper or warmer in the EEP (5, 10). This effect applied to longer time scales may explain why permanent El Niño conditions during the Pliocene were accompanied by reduced-amplitude glacial-interglacial cycles; a deeper or warmer thermocline may have preconditioned the tropical system such that air-sea feedbacks needed to amplify small perturbations in solar forcing were weak. The establishment of Walker circulation at ~1.7 Ma coincides with the Pliocene-Pleistocene epoch boundary, after which the sensitivity of climate to solar forcing peaked (16).

Our study indicates that today's zonally asymmetric SST pattern and thermocline structure of the tropical Pacific are not stable over long time scales. Given the importance of tropical Pacific processes in modulating meriodional heat transport, these results indicate that in a warmer world, the ocean may accomplish redistribution of heat in a fundamentally different way. Thus, the Pliocene warm period provides a target and a test to climate models and theory and is an indication that climate feedbacks do not work to maintain the presently strong asymmetry across the Pacific under some circumstances. It may indicate that warming cannot continue indefinitely without substantial changes in the Walker circulation (10) and that changes in the subtropics, communicated through the thermocline, might cause a fundamental reorganization of the tropical Pacific ocean-atmosphere system (4, 10). Depending on one's interpretation of the instrumental data from the tropical Pacific, a shift in the baseline tropical Pacific pattern may already be occurring (2, 4, 5, 8).

References and Notes

1. M. A. Cane, *Science* **282**, 59 (1998).
2. M. J. McPhaden, D. Zhang, *Nature* **415**, 603 (2002).
3. U. Cubasch *et al.*, in *Climate Change 2001, The Scientific Basis*, J. T. Houghton, Y. Ding, Eds. (Cambridge Univ. Press, New York, 2001), pp. 525–582.
4. A. V. Fedorov, S. G. H. Philander, *J. Clim.* **14**, 3086 (2001).
5. A. V. Fedorov, S. G. Philander, *Science* **288**, 1997 (2000).
6. D. S. Battisti, A. C. Hirst, *J. Atmos. Sci.* **46**, 1687 (1989).
7. D.-E. Sun, T. Zhang, S.-I. Shin, *J. Clim.* **17**, 3786 (2004).
8. K. E. Trenberth, J. M. Caron, D. P. Stepaniak, S. Worley, *J. Geophys. Res.* **107**, 10.1029/2000JD000298 (2002).
9. D.-E. Sun, *J. Clim.* **16**, 185 (2003).
10. D.-E. Sun, J. Fasullo, T. Zhang, A. Roubicek, *J. Clim.* **16**, 2425 (2003).
11. G. Boccaletti, R. C. Pacanowski, S. G. H. Philander, A. V. Fedorov, *J. Phys. Oceanogr.* **34**, 888 (2004).
12. A. V. Fedorov, R. C. Pacanowski, S. G. H. Philander, G. Boccaletti, *J. Phys. Oceanogr.* **34**, 1949 (2004).
13. K. B. Rodgers, P. Friederichs, M. Latif, *J. Clim.* **17**, 3761 (2004).
14. A. Timmermann, *Global Planet. Change* **37**, 135 (2003).
15. M. A. Cane, *Earth Planet. Sci. Lett.* **230**, 227 (2005).
16. A. C. Ravelo, D. H. Andreasen, M. Lyle, A. O. Lyle, M. W. Wara, *Nature* **429**, 263 (2004), and references therein.
17. J. H. Yin, D. S. Battisti, *J. Clim.* **14**, 565 (2001).
18. P. S. Dekens, D. W. Lea, D. K. Pak, H. J. Spero, *Geochem. Geophys. Geosystems* **3**, 1022 (2002).
19. Materials and methods are available as supporting material on *Science* Online.
20. R. E. M. Rickaby, P. Halloran, *Science* **307**, 1948 (2005).
21. A. M. Haywood, P. Dekens, A. C. Ravelo, M. Williams, *Geochem. Geophys. Geosyst.* **6**, 10.1029/2004GC000799 (2005).
22. K. Cannariato, A. C. Ravelo, *Paleoceanography* **12**, 805 (1997).
23. A. C. Ravelo, M. W. Wara, *Oceanography* **17**, 22 (2004).
24. A. C. Ravelo, R. G. Fairbanks, *Paleoceanography* **7**, 815 (1992).
25. D. J. Andreasen, A. C. Ravelo, *Paleoceanography* **12**, 395 (1997).
26. We use a sensitivity of foraminiferal calcite ^{18}O to temperature of 0.21‰ δ^{18}O per °C from (35).
27. W. Chaisson, A. C. Ravelo, *Paleoceanography* **15**, 497 (2000).
28. S. G. H. Philander, A. V. Fedorov, *Paleoceanography* **18**, 1045 10.1029/2002PA000837 (2003).
29. F. B. Schwing, T. Murphee, P. M. Green, *Prog. Oceanogr.* **53**, 115 (2002).
30. P. Molnar, M. A. Cane, *Paleoceanography* **17**, 11-1 (2002).
31. H. Dowsett, J. Barron, R. Poore, *Mar. Micropaleontology* **27**, 13 (1996).
32. J. R. Marlow, C. B. Lange, G. Wefer, A. Roselle-Melé, *Science* **290**, 2288 (2000).
33. Although a detailed study of *G. tumida* needs to be performed, a low-resolution record of Mg/Ca measurements of *G. tumida* from the same site location (ODP site 847) shows cooling of the subsurface before 3.5 Ma (20), implying that our use of δ^{18}O of *G. tumida* as an indicator of temperature is appropriate and that changes in the δ^{18}O of seawater are probably negligible.
34. J. Bjerknes, *Mon. Weather Rev.* **97**, 163 (1969).
35. B. E. Bemis, H. J. Spero, J. Bjima, D. W. Lea, *Paleoceanography* **13**, 150 (1998).
36. E. Kalnay *et al.*, *Bull. Am. Meteorol. Soc.* **77**, 437 (1996).
37. Data are available at www.cdc.noaa.gov.
38. We thank M. Cane, G. Philander, A. Fedorov, and P. Molnar for helpful discussions; R. Franks for analytical support; and A. Schilla, C. Ziegler, and M. Flower for help with sample preparation and analysis. We thank the Ocean Drilling Program (ODP) for supplying samples. The ODP is sponsored by NSF and participating countries under the management of Joint Oceanographic Institutions (JOI), Incorporated. We thank NSF (grant to A.C.R.) for funding this work. Requests for data should be sent to A.C.R.

Embryos of an Early Jurassic Prosauropod Dinosaur and Their Evolutionary Significance

Robert R. Reisz,[1]* Diane Scott,[1] Hans-Dieter Sues,[2] David C. Evans,[1] Michael A. Raath[3]

Articulated embryos from the Lower Jurassic Elliot Formation of South Africa are referable to the prosauropod *Massospondylus carinatus* and, together with other material, provide substantial insights into the ontogenetic development in this early dinosaur. The large forelimbs and head and the horizontally held neck indicate that the hatchlings were obligate quadrupeds. In contrast, adult *Massospondylus* were at least facultatively bipedal. This suggests that the quadrupedal gait of giant sauropods may have evolved by retardation of postnatal negative allometry of the forelimbs. Embryonic body proportions and an absence of well-developed teeth suggest that hatchlings of this dinosaur may have required parental care.

Prosauropod dinosaurs appeared during the early Late Triassic (1, 2) and became the dominant large herbivores in Late Triassic and Early Jurassic continental ecosystems (3) [220 to 183 million years ago (Ma)]. The prosauropod *Massospondylus carinatus* Owen, 1854 is known from numerous well-preserved specimens from many localities in the Lower Jurassic Elliot and Clarens formations of South Africa and Lesotho (4, 5). It is represented by many articulated skeletons that form an extensive growth series. Here we describe articulated embryonic skeletons referable to *Massospondylus* and provide evidence that the quadrupedal gait in sauropods may have evolved through paedomorphosis.

A cluster of six subspherical eggs (6 cm in maximum diameter) was collected from the *Massospondylus* Range Zone of the upper Elliot Formation in Golden Gate Highlands National Park in South Africa (6, 7). During preparation, we identified embryonic skeletal material in the bottom halves of five of the eggs; the sixth egg seems to have hatched.

[1]Department of Biology, University of Toronto at Mississauga, Mississauga, ON L5L 1C6, Canada. [2]Department of Paleobiology, National Museum of Natural History, Smithsonian Institution, Washington, DC 20013–7012, USA. [3]Bernard Price Institute for Palaeontological Research, University of the Witwatersrand, Wits 2050, Johannesburg, South Africa.

*To whom correspondence should be addressed. E-mail: rreisz@utm.utoronto.ca